NeuroImage: Clinical 8 (2015) 448–454

Contents lists available at ScienceDirect

NeuroImage: Clinical

journal homepage: www.elsevier.com/locate/ynicl

# [18F]-fluoro-L-thymidine PET and advanced MRI for preoperative grading of gliomas

S. Collet[a,b,c,d], S. Valable[a,b,c,d], J.M. Constans[a,b,c,d,e], E. Lechapt-Zalcman[a,b,c,d,f], S. Roussel[a,b,c,d], N. Delcroix[g,h], A. Abbas[k,l,m,n], M. Ibazizene[a,b,c,d], M. Bernaudin[a,b,c,d], L. Barré[a,b,c,d], J.M. Derlon[a,b,c,d,i], J.S. Guillamo[a,b,c,d,j,*]

[a]CNRS, UMR 6301 ISTCT, CERVOxy ou LDM-TEP ou ISTS group, GIP CYCERON, Caen F-14074, France
[b]CEA, DSV/I2BM, UMR 6301 ISTCT, Caen F-14074, France
[c]Université de Caen Basse-Normandie, UMR 6301 ISTCT, Caen F-14074, France
[d]Normandie Univ, France
[e]CHU de Caen, Service de Neuroradiologie, Caen F-14000, France
[f]CHU de Caen, Service d'Anatomie Pathologie, Caen F-14000, France
[g]CNRS, UMS 3408, GIP CYCERON, Caen F-14074, France
[h]Université de Caen Basse-Normandie, UMS 3408, Caen F-14074, France
[i]CHU de Caen, Service de neurochirurgie, Caen F-14000, France
[j]CHU de Caen, Service de Neurologie, Caen F-14000, France
[k]Inserm, Caen U1077, France
[l]Université de Caen Basse-Normandie UMR, Caen-S1077, France
[m]École Pratique des Hautes Etudes, UMR, Caen-S1077, France
[n]CHU de Caen, Caen U1077, France

ARTICLE INFO

*Article history:*
Received 27 March 2015
Received in revised form 5 May 2015
Accepted 25 May 2015
Available online 29 May 2015

*Keywords:*
Glioma
Glioblastoma
Grading
MRI
MR spectroscopy
[18F]-FLT-PET

ABSTRACT

*Purpose:* Conventional MRI based on contrast enhancement is often not sufficient in differentiating grade II from grade III and grade III from grade IV diffuse gliomas. We assessed advanced MRI, MR spectroscopy and [18F]-fluoro-L-thymidine ([18F]-FLT) PET as tools to overcome these limitations.
*Methods:* In this prospective study, thirty-nine patients with diffuse gliomas of grades II, III or IV underwent conventional MRI, perfusion, diffusion, proton MR spectroscopy (1H-MRS) and [18F]-FLT-PET imaging before surgery. Relative cerebral blood volume (rCBV), apparent diffusion coefficient (ADC), Cho/Cr, NAA/Cr, Cho/NAA and FLT-SUV were compared between grades.
*Results:* Cho/Cr showed significant differences between grade II and grade III gliomas ($p = 0.03$). To discriminate grade II from grade IV and grade III from grade IV gliomas, the most relevant parameter was the maximum value of [18F]-FLT uptake $FLT_{max}$ (respectively, $p < 0.001$ and $p < 0.0001$). The parameter showing the best correlation with the grade was the mean value of [18F]-FLT uptake $FLT_{mean}$ ($R^2 = 0.36$, $p < 0.0001$) and $FLT_{max}$ ($R^2 = 0.5$, $p < 0.0001$).
*Conclusion:* Whereas advanced MRI parameters give indications for the grading of gliomas, the addition of [18F]-FLT-PET could be of interest for the accurate preoperative classification of diffuse gliomas, particularly for identification of doubtful grade III and IV gliomas.


## 1. Introduction

Diffuse gliomas are the most common primary brain tumors in adults and encompass a heterogeneous group of tumors with different histopathological features, aggressiveness, imaging, response to treatment and survival.

They are primarily defined by the histopathological tumor tissue analysis and subdivided by the World Health Organization (WHO) classification into grade II (low grade glioma), grade III (anaplastic glioma) and grade IV (glioblastoma multiforme, GBM).

Accurate distinction between different grades is of significant clinical importance because of its strong prognostic and treatment decision-making implications (Louis et al., 2007). However, histopathological criteria of the grading system present some limitations such as the lack of reproducibility and the prognostic heterogeneity within the same group (Ricard et al., 2012). To improve this classification, some molecular markers not only have diagnostic and prognostic implications, but also therapeutic efficacy prediction (1p/19q co-deletion, IDH1/IDH2 mutations and MGMT promoter methylation) (Riemenschneider et al., 2010). However, these approaches require a resection or a biopsy and

* Corresponding author at: Service de Neurologie, Caen F-14033, France. Tel.: +33 2 31 06 46 17; fax: +33 2 31 06 51 16.
*E-mail address:* guillamo-js@chu-caen.fr (J.S. Guillamo).

http://dx.doi.org/10.1016/j.nicl.2015.05.012

have limitations induced by intra-tumoral heterogeneity (van den Bent, 2010). Furthermore, there is a need to identify criteria of aggressiveness for inoperable patients.

MRI is a part of the daily management of the patients by providing anatomical and vascular information. The presence or the absence of T1 enhancement after gadolinium-chelate injection, necrosis, mass effect and surrounding tumor edema are established parameters used in characterizing tumor aggressiveness (Dean et al., 1990). The presence of contrast enhancement in diffuse glioma, related to the permeability of the blood–brain-barrier (BBB) reflecting neovascularization, is often regarded as a sign of malignancy. However, it presents some limitations and does not allow for reliable separation between different grades. For example, although the absence of contrast enhancement is a commonly used criterion for identifying grade II gliomas, it does not eliminate formally a malignant tumor (Ginsberg et al., 1998; Scott et al., 2002). In contrast, the presence of contrast enhancement and even necrosis, characteristic of GBM, can be observed in pure grade III oligodendrogliomas.

In this context, multimodal imaging based on MRI and PET parameters, by assessing tumor pathophysiology such as microvasculature, metabolism, proliferation or cellularity, could be of additional value.

Previous reports have described and compared the performance of glioma grading using advanced MRI techniques such as relative cerebral blood volume (rCBV), apparent diffusion coefficient (ADC), and metabolites of Magnetic Resonance Spectroscopy (MRS) (Arvinda et al., 2009; Hilario et al., 2012; Law et al., 2003; van den Bent, 2010; Yang et al., 2002; Zonari et al., 2007; Zou et al., 2011). Others focus specifically on glioma grading with the thymidine analog [$^{18}$F]-fluoro-L-thymidine ([$^{18}$F]-FLT), developed as a positron emission tomography (PET) tracer to assess the proliferation activity of tumors in vivo, particularly in brain tumors (Chalkidou et al., 2012; Chen et al., 2005; Hatakeyama et al., 2008; Jacobs et al., 2005). Even if these multimodal imaging parameters are useful to distinguish grade II from higher grades (anaplastic and GBM), the differentiating criteria of grade III from grade IV gliomas, two groups with different prognoses and management, are still poorly defined.

The aim of this study was to compare the performance of these advanced MR techniques, namely perfusion, diffusion and proton MR spectroscopy ($^{1}$H-MRS) with that of [$^{18}$F]-FLT-PET, by pre-operatively assessing the diagnostic accuracy of each parameter in differentiating glioma grades.

## 2. Methods

### 2.1. Patients

This study was based on a prospective clinical trial funded by INCa (Institut National du Cancer) and approved by the local ethics committee and AFSSAPS agreement (ClinicalTrials.gov identifier: NCT00850278). Forty patients were included in the Caen University Hospital. Inclusion criteria were: a presumed diffuse glioma amenable to surgical resection or biopsy, age greater than or equal to 18, KPS greater than or equal to 50, normal blood cell count, normal biological hepatic functions and a signed informed consent. The group sizes of the different tumor grades were the result of the incidence of each tumor in this prospective study. Patients first underwent [$^{18}$F]-FLT-PET, followed by multiparametric MRI/MRS within the same week and prior to surgery. Single voxel MRS was localized in the area with maximum visible uptake of [$^{18}$F]-FLT. Thereafter, patients underwent surgery, resection or biopsy depending on the location of the tumor, and the specimens were histopathologically evaluated by an experienced neuropathologist (ELZ). Majority of patients had image-guided total or subtotal surgical resection (Table 1). For patients with biopsy only, the biopsy was guided by the area with maximum visible uptake of [$^{18}$F]-FLT. For grade III tumors or for difficult cases, the diagnosis and grading were reviewed by the national multicentric network "Prise en charge des OLigodendrogliomes Anaplasiques POLA" (Idbaih et al., 2012).

### 2.2. Image acquisition

*MR imaging* was performed on a 1.5 Tesla GEMS version HDXt 15.0. After scout-view and coronal T2-weighted imaging, an axial FLAIR (Fluid Attenuated Inversion Recovery) sequence was performed (24 slices, slice spacing 5.5, pixel resolution 0.47 × 0.47 mm, TR/TE = 9602/150 ms). Diffusion Weighted Imaging (DWI) was performed using Spin-Echo-Echo Planar Imaging (SE-EPI) (3 diffusion directions, 36 slices, slice spacing: 7 mm, pixel resolution: 1.09 × 1.09 mm, TR/TE = 6000/96 ms, b ≈ 0 and b ≈ 1000 s•mm$^2$). For perfusion, dynamic T2*-weighted EPI images were acquired 30 s before, during the first pass of Gd-DOTA (Dotarem®, Guerbet, France) and 1 min after with a standard 0.1 mmol/kg body weight dose (14 slices, 35 repetitions, slice spacing: 7 mm, pixel resolution 2.19 × 2.19 mm, TR/TE = 2280/60 ms). Immediately thereafter, a 3DT1-weighted sequence, 3DT1w-Gd (124 slices, slice spacing 1.5, pixel resolution 1.01 × 1.01 mm, TR/TE = 17/3 ms) was performed to evaluate the tumor contrast enhancement. Finally, MRS data were acquired in a single voxel (1 cm$^3$) localized in the tumor in the area of maximal uptake of FLT and in the normal-appearing contralateral side with PRESS MRS sequence with multiple TE (35, 144, 288 ms) and water suppression.

*FLT-PET* [$^{18}$F]-FLT was produced by the LDM-TEP group and synthesized at the CYCERON TEP center as previously described by Jacobs et al. (2005). Acquisitions were performed on a General Electric Discovery VCT 64 PET scanner. Images of the brain were acquired 40 min after the intravenous injection of 5 MBq/kg of $^{18}$F-FLT and lasted 10 min, to match a clinically feasible approach. The attenuation-corrected images were reconstructed with an OSEM 2D algorithm (9 subsets and 2 iterations) and filtered in 3D with a Butterworth filter.

### 2.3. Image analysis

*ADC maps* were computed from DWI. The ADC (apparent diffusion coefficient) maps were calculated pixel-by-pixel using ImageJ software (http://rsb.info.nih.gov/ij/, 1997–2012) using the following equation: $ADC = -[\ln(S/S_0)]/b$ where S is the signal (averaged over the 3 directions) acquired, b = 1000, and $S_0$ = the signal acquired without diffusion gradient. Values were expressed as $10^{-6}$ mm$^2$/s. r*CBV maps* were computed using perfusion imaging. Variations of the T2* signal in the tissue, which is proportional to the concentration of the contrast agent, were calculated with in-house macros based on ImageJ software as: $\Delta R^{2^*}(t) = -\ln(S(t)/S_0)$, where $S_0$ = the signal intensity before contrast agent injection, and S(t) = the signal intensity over time. Then, CBV maps were generated by integrating the area under the γ-variate fitted curves to avoid an effect of recirculation. Images were then normalized by dividing CBV maps with the mean value of the normal-appearing contralateral side. *Coregistration:* ADC maps, rCBV maps, FLAIR and PET-FLT images were coregistered with trilinear interpolation, rigid matching and normalized mutual information on 3DT1w-Gd images (PMOD 3.1® software).

### 2.4. ROI segmentation

The hypersignal in FLAIR images was manually delineated to define a Region Of Interest (ROI) in order to use a homogeneous method to define a pathological area (tumor, peripheral edema and infiltration areas) for the different grades, despite the presence or absence of T1 enhancement. When present, necrosis was excluded.

### 2.5. Parameter extraction

Tumor ROIs were reported for each modality (rCBV, ADC, T1 enhancement, FLT-PET) to extract the mean value for each modality, the

**Table 1**
Patients and tumor characteristics (GGII: glioma grade II, GGIII: glioma grade III, GGIV: glioma grade IV, M: male, F: female, R: right, L: left, CC: corpus callosum, CE: contrast enhancement after gadolinium injection, nec: necrosis, Yes: 1, No: 0, EOR: extent of resection, PE: partial resection, CR: complete resection, B: biopsy, NA: not available).

| Patient | Sex | Age | KPS | Tumor location | CE | Nec | EOR | WHO grade | Pathological diagnosis |
|---|---|---|---|---|---|---|---|---|---|
| 1 | F | 55 | 100 | Frontal, L | 0 | 0 | PR | 2 | Oligodendroglioma |
| 2 | M | 62 | NA | Temporal, R | 0 | 0 | CR | 2 | Oligodendroglioma |
| 3 | F | 53 | 100 | Temporal, L | 0 | 0 | CR | 2 | Oligodendroglioma |
| 4 | F | 60 | NA | Frontal, R | 0 | 0 | CR | 2 | Oligodendroglioma |
| 5 | M | 38 | 100 | Frontal, L | 0 | 0 | PR | 2 | Oligodendroglioma |
| 6 | F | 44 | 100 | Parietal, temporal, R | 0 | 0 | PR | 2 | Oligodendroglioma |
| 7 | F | 27 | 100 | Central | 0 | 0 | PR | 2 | Oligodendroglioma |
| 8 | F | 60 | 90 | CC | 1 | 0 | CR | 3 | Oligodendroglioma |
| 9 | F | 41 | 90 | Frontal, R | 1 | 0 | CR | 3 | Oligodendroglioma |
| 10 | F | 29 | 100 | Parietal, L | 0 | 0 | CR | 3 | Oligoastrocytoma |
| 11 | F | 25 | 100 | Frontal, L | 0 | 0 | CR | 3 | Oligoastrocytoma |
| 12 | F | 48 | NA | Frontal, L | 0 | 0 | CR | 3 | Oligodendroglioma |
| 13 | M | 47 | 80 | Temporal, insular, R | 1 | 0 | B | 3 | Oligodendroglioma |
| 14 | F | 46 | 90 | Frontal, L | 0 | 0 | CR | 3 | Oligodendroglioma |
| 15 | M | 50 | 90 | frontal, temporal, insular, L | 1 | 1 | PR | 3 | Astrocytoma |
| 16 | F | 38 | 100 | Temporal, R | 1 | 1 | CR | 3 | Oligodendroglioma |
| 17 | M | 58 | 80 | Parietal, occipital, R | 1 | 1 | PR | 4 | Glioblastoma |
| 18 | F | 74 | 80 | Parietal, temporal, occipital, L | 1 | 1 | CR | 4 | Glioblastoma |
| 19 | M | 73 | 80 | Frontal, parietal, temporal, R | 1 | 1 | CR | 4 | Glioblastoma |
| 20 | M | 59 | 80 | Frontal, R | 1 | 0 | CR | 4 | Glioblastoma |
| 21 | M | 70 | 100 | Parietal, central, L | 1 | 1 | CR | 4 | Glioblastoma |
| 22 | F | 44 | 70 | Frontal, bilateral, multifocal | 1 | 1 | B | 4 | Glioblastoma |
| 23 | F | 46 | 80 | Frontal, CC, L | 1 | 1 | PR | 4 | Glioblastoma |
| 24 | M | 52 | 80 | Parietal, L | 1 | 1 | CR | 4 | Glioblastoma |
| 25 | F | 70 | 80 | Frontal, occipital, multifocal | 1 | 1 | B | 4 | Glioblastoma |
| 26 | M | 24 | 100 | Frontal, temporal | 1 | 1 | CR | 4 | Glioblastoma |
| 27 | M | 52 | 80 | Frontal, R | 1 | 1 | CR | 4 | Glioblastoma |
| 28 | F | 64 | 80 | Frontal, parietal, CC, multifocal, L | 1 | 1 | B | 4 | Glioblastoma |
| 29 | M | 28 | 100 | Parietal, temporal, insular, L | 1 | 1 | PR | 4 | Glioblastoma |
| 30 | M | 58 | 90 | temporal, R | 1 | 1 | CR | 4 | Glioblastoma |
| 31 | M | 79 | 80 | Frontal, bilateral | 1 | 1 | B | 4 | Glioblastoma |
| 32 | M | 67 | 80 | Occipital | 1 | 1 | B | 4 | Glioblastoma |
| 33 | M | 53 | 70 | Frontal, multifocal | 1 | 1 | B | 4 | Glioblastoma |
| 34 | M | 64 | 80 | Frontal, L | 1 | 1 | CR | 4 | Glioblastoma |
| 35 | M | 52 | 80 | Frontal, R | 1 | 1 | PR | 4 | Glioblastoma |
| 36 | M | 74 | 80 | Frontal, parietal, L | 1 | 1 | CR | 4 | Glioblastoma |
| 37 | M | 72 | 60 | Frontal, CC, bilateral, multifocal | 1 | 1 | B | 4 | Glioblastoma |
| 38 | M | 62 | 80 | Occipital, CC, L | 1 | 1 | PR | 4 | Glioblastoma |
| 39 | M | 67 | 90 | Temporal, insular, R | 1 | 1 | B | 4 | Glioblastoma |

maximum value for rCBV, CE and PET-FLT, and the minimum value for ADC. To avoid sensitivity to extreme values, the minimum value was associated with the 10th percentile (p10) and the maximum value with the 90th percentile (p90). In MRS, choline (Cho), creatine (Cr), N-Acethyl-Aspartate (NAA), phospholipids and lactate were quantified with SA/GE software (GE) to obtain peak amplitudes and areas (proportional to concentration and relaxation) from spectra with water resonance suppression, and expressed as a ratio.

### 2.6. Statistical analysis

Statistical analyses were performed with JMP© software. Analysis was performed between all grades. *p*-Values of comparisons between grades were calculated using the non-parametric Wilcoxon test. A *p*-value $< 0.05$ was considered statistically significant. Ordinal logistic regression was used to assess the degree of correlation ($R^2$) of each parameter with the grade. Only $R^2$ values with *p*-value $< 0.05$ were considered significant.

## 3. Results

### 3.1. Patients and tumor characteristics

Among the 40 patients included in the study, 1 had an incomplete MRI examination. Of the 39 remaining patients, all presented histopathologically proven diffuse glioma based on WHO criteria and were eligible in the final analysis (ranging from 21 to 79 years old, 17 women and 22 men). The diagnosis was established from biopsy specimens ($n = 9$) or from resection (10 patients with a partial resection and 20 patients with a macroscopically complete resection) yielding 7 patients with grade II glioma, 9 patients with grade III glioma and 23 patients with grade IV glioma. Table 1 shows patients and tumor characteristics.

### 3.2. Interest of multimodal imaging at the individual level

Fig. 1 illustrates the multimodal imaging of tumors of each grade. Grade II gliomas typically looked like a non-enhancing lesion that had no modification on CBV maps and no [$^{18}$F]-FLT uptake (Fig. 1). Most grade III gliomas showed a slightly enhancing lesion with mild [$^{18}$F]-FLT uptake (Fig. 1: Grade III (a)). In contrast, grade IV gliomas typically exhibited a strong contrast enhancement, elevated rCBV, and high [$^{18}$F]-FLT uptake (Fig. 1: Grade IV (a)). Interestingly, some grade III glioma presented a profile indicative of a GBM, i.e. sustained contrast enhancement, strong modification in ADC, elevated Cho/Cr and rCBV, appearance of lipids/lactate but [$^{18}$F]-FLT clearly demonstrated a weak tumor cell proliferation (Fig. 1: Grade III (b)).

On the opposite, a grade IV glioma presented non-objectivable modification in perfusion but an intense [$^{18}$F]-FLT uptake favoring the diagnosis of a GBM instead of a grade III glioma (Fig. 1: Grade IV (b)).

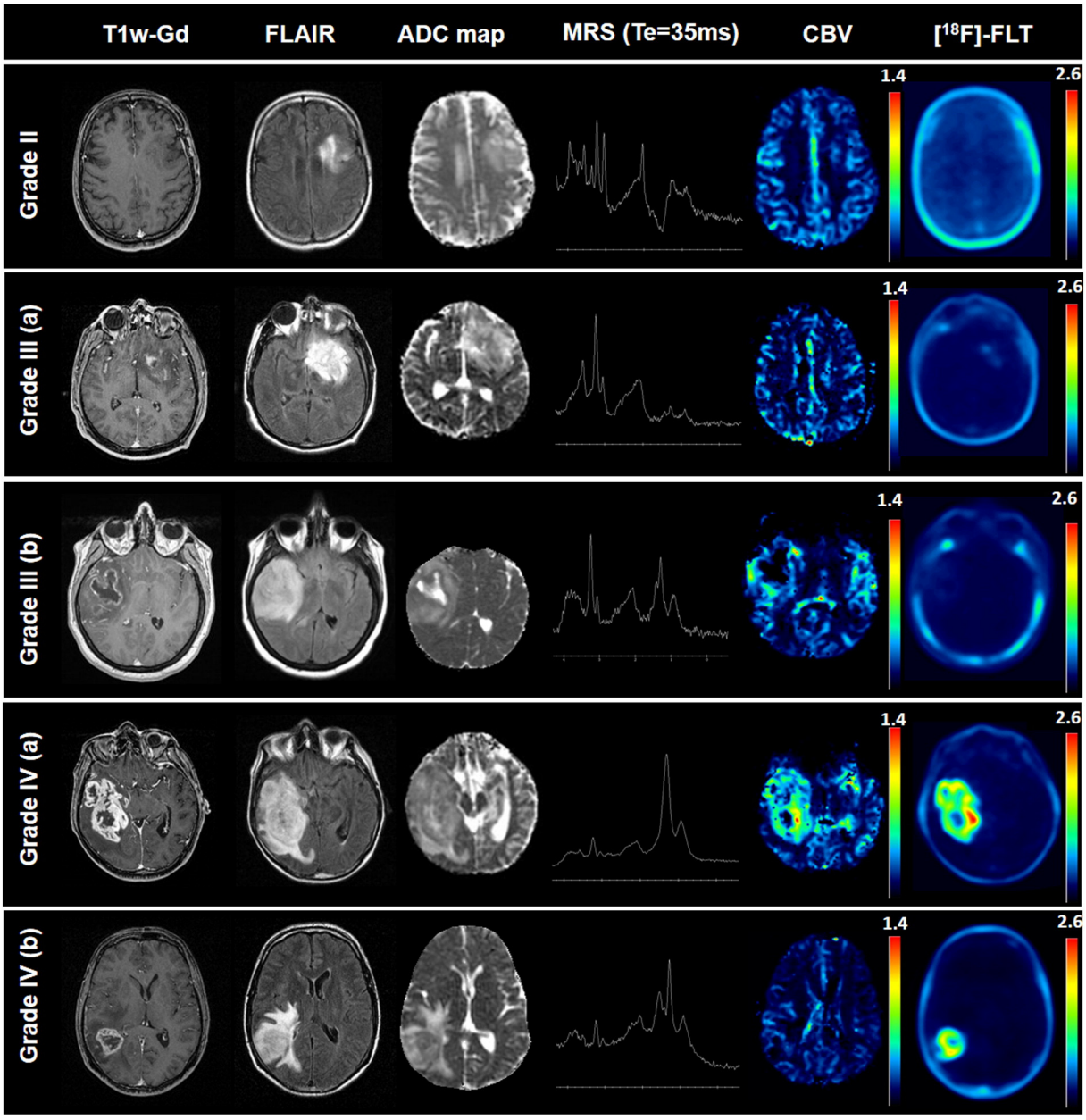


**Fig. 1.** Multimodal aspect on imaging of a patient with a grade II glioma, two patients with a grade III glioma and two patients with a grade IV glioma.

### 3.3. Comparisons of imaging parameters between grades

Between grade II and grade IV gliomas $rCBV_{mean}$, $rCBV_{max}$, $FLT_{mean}$, $FLT_{max}$, $CE_{mean}$, $CE_{max}$, Cho/Cr and Cho/NAA showed significant differences (Table 2). The most relevant parameter was $FLT_{max}$ ($p < 0.001$) (Fig. 2, Table 2).

Between grade III and grade IV gliomas, $ADC_{mean}$, $ADC_{min}$, $rCBV_{mean}$, $rCBV_{max}$, $FLT_{mean}$, $FLT_{max}$, $CE_{mean}$, and $CE_{max}$ showed significant

**Table 2**
Quantification of imaging parameters for grade II gliomas ($n = 7$), grade III gliomas ($n = 9$) and grade IV ($n = 23$). $p$-Values from the Wilcoxon test, values of $R^2$ with significant $p$-value from a logistic regression analysis between the grade and the parameters (NS: not significant).

| | Grade II (mean ± SD) | Grade III (mean ± SD) | Grade IV (mean ± SD) | Wilcoxon test ($p$-value) | | | Logistic regression | |
|---|---|---|---|---|---|---|---|---|
| | | | | II/III | III/IV | II/IV | $R^2$ | $p$-Value |
| $ADC_{mean}$ ($10^{-6}$ $mm^2/s$) | 1201 ± 89 | 1345 ± 130 | 1176 ± 129 | NS | 0.013 | NS | 0.04 | NS |
| $ADC_{min}$ ($10^{-6}$ $mm^2/s$) | 903 ± 66 | 962 ± 55 | 837 ± 71 | NS | <0.001 | NS | 0.15 | <0.01 |
| $rCBV_{mean}$ | 1.18 ± 0.19 | 1.11 ± 0.35 | 1.59 ± 0.43 | NS | 0.010 | 0.035 | 0.15 | <0.01 |
| $rCBV_{max}$ | 1.88 ± 0.37 | 1.77 ± 0.52 | 2.73 ± 0.68 | NS | <0.01 | 0.013 | 0.21 | <0.001 |
| Cho/Cr | 1.41 ± 0.20 | 3.71 ± 4.04 | 3.65 ± 1.97 | 0.03 | NS | <0.01 | 0.03 | NS |
| NAA/Cr | 1.15 ± 0.28 | 0.85 ± 0.40 | 0.89 ± 0.33 | NS | NS | NS | 0.01 | NS |
| Cho/NAA | 1.18 ± 0.41 | 4.91 ± 4.66 | 3.84 ± 2.44 | NS | NS | 0.021 | 0.01 | NS |
| $FLT_{mean}$ (g/ml) | 0.27 ± 0.09 | 0.25 ± 0.09 | 0.61 ± 0.23 | NS | <0.001 | <0.01 | 0.36 | <0.0001 |
| $FLT_{max}$ (g/ml) | 0.34 ± 0.09 | 0.33 ± 0.14 | 1.27 ± 0.56 | NS | <0.0001 | <0.001 | 0.5 | <0.0001 |

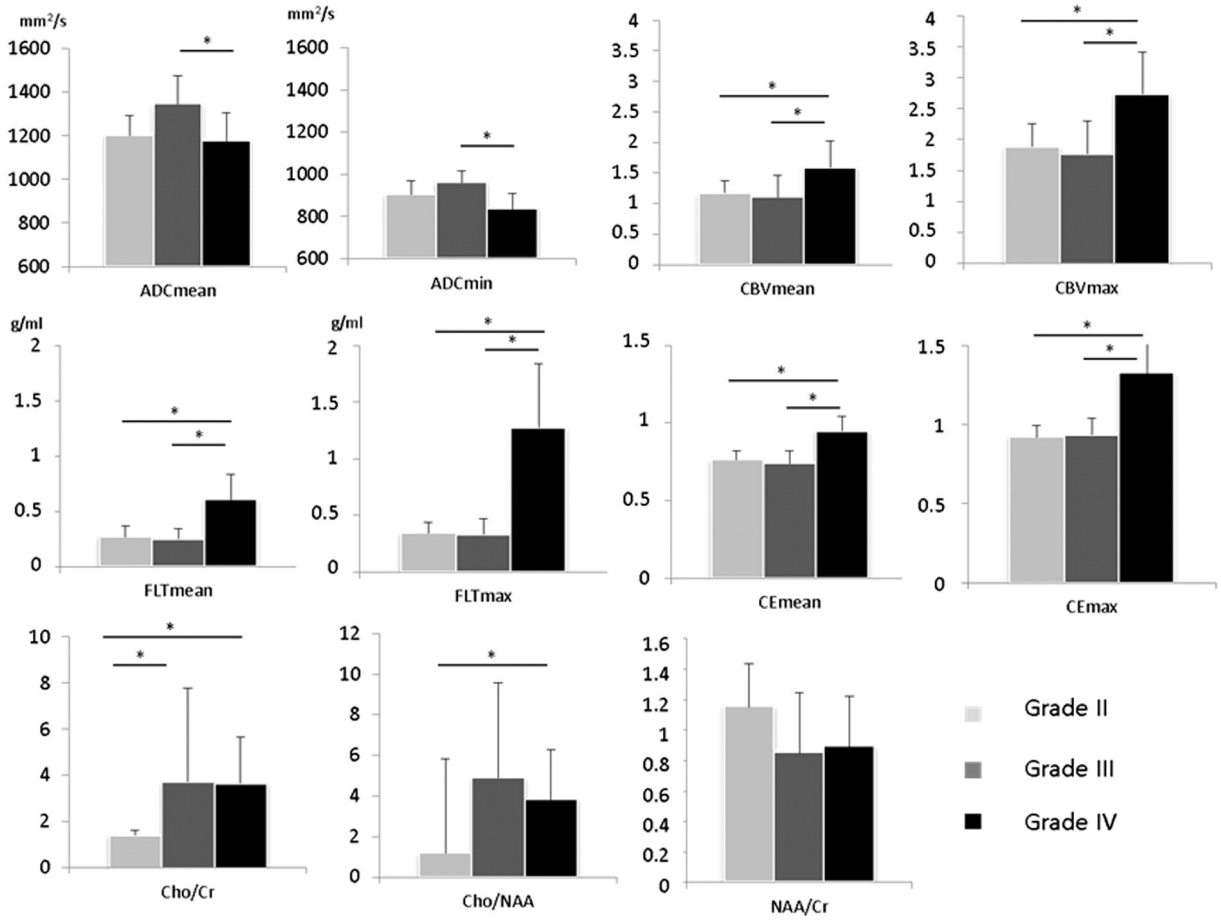


**Fig 2.** Graphic representation of the parameters used to distinguish between grade II gliomas ($n = 7$), grade III gliomas ($n = 9$) and grade IV gliomas ($n = 23$).

differences (Table 2). The most relevant parameter was $FLT_{max}$ ($p < 0.0001$) (Fig. 2, Table 2). Cho/Cr showed significant differences between grade II and grade III gliomas ($p = 0.03$).

The parameter showing the best significant correlation with the grade was $FLT_{max}$ ($R^2 = 0.5$, $p < 0.0001$) (Table 2).

## 4. Discussion

The prognosis and management of patients with diffuse glioma are strongly dependent on the accurate grading of the tumor. MRI plays a crucial role in the assessment of aggressiveness of gliomas before surgery but may remain insufficient to forecast prognosis of diffuse gliomas. Therefore, multimodal imaging parameters with advanced MRI (CBV and ADC), MRS and [$^{18}$F]-FLT-PET could identify relevant markers to better predict the grading of gliomas.

Among advanced technics, Cho/Cr ratio presented interesting performances for the discrimination of different grades. This was also shown in our study, particularly between grade II and grade III gliomas ($p = 0.03$). Indeed, Cho/Cr is well known to be correlated with tumor cell proliferation (Herminghaus et al., 2002) and usually presents significant differences between low grade and high grade gliomas (Law et al., 2003; Server et al., 2011; Yang et al., 2002; Zou et al., 2011). Our results suggest that the use of Cho/Cr ratio could be of interest in the management of grade II and grade III rather than [$^{18}$F]-FLT PET, that did not show significant differences between these grades. rCBV has been shown to be correlated with tumor aggressiveness and with grade in enhancing and in non-enhancing lesions (Aronen et al., 1994; Lev et al., 2004; Maia et al., 2005; Sadeghi et al., 2008; Shin et al., 2002; Sugahara et al., 1998). rCBV has a better diagnostic performance in differentiating between low grade and high grade gliomas than Cho/Cr and Cho/NAA ratios obtained with MRS (Law et al., 2003), ADC (Arvinda et al., 2009) or Ktrans (Law et al., 2004). While most studies compare high grade and low grade, our study suggests that $CBV_{mean}$ and $CBV_{max}$ significantly differ between patients with grade III and patients with grade IV. For Zonari et al., rCBV is the most important parameter for accurate tumor grading by differentiating grade II from III gliomas (Zonari et al., 2007).

Along with [$^{18}$F]-FDG, numerous other PET radiotracers have been developed (for review, see (Dhermain et al., 2010; Wester, 2007)) to assess tumor aggressiveness such as 3′-[$^{18}$F]fluoro-3′-deoxy-L-thymidine ([$^{18}$F]-FLT) (Jacobs et al., 2005) or amino acid metabolism by *o*-(2-[$^{18}$F]fluoroethyl)-L-tyrosine ([$^{18}$F]-FET) (Hutterer et al., 2011) or methyl-[$^{11}$C]-L-methionine ([$^{11}$C]-MET) (Derlon et al., 2000). Among these tracers, [$^{18}$F]-FLT correlates with cell proliferation, particularly in brain tumors (Chalkidou et al., 2012). This tracer has already been used by us and others to assess grade (Ferdová et al., 2015), treatment efficacy (Corroyer-Dulmont et al., 2013; Schwarzenberg et al., 2012) or prognosis (Idema et al., 2012). [$^{18}$F]-FLT has also been assessed and compared with other tracers as a marker for high grade gliomas and probably more adapted for the grading compared to [$^{11}$C]-MET or [$^{18}$F]-FET in this setting (Chen et al., 2005; Hatakeyama et al., 2008; Jacobs et al., 2005; Jeong and Lim, 2012; Miyake et al., 2012). In agreement with these reports, our study showed that [$^{18}$F]-FLT parameters were not sensitive enough to distinguish grade II from grade III gliomas, but was the best parameter to distinguish grade IV from lower grade gliomas. Our results are in line of previous work that already showed the interest of using [$^{18}$F]-FLT to differentiate low and high grade gliomas (Yamamoto et al., 2012). We are also aware that PET imaging and more precisely FLT PET are restricted, at the present time, to few hospital or research centers. In the present study, we propose that FLT PET

adds information in presence of suspicious patients where MRI may be not sensitive enough before any treatment is decided but where biopsy examination may lose some very aggressive "hot spot" thanks to the great spatial heterogeneity.

Of note, we chose a static and delayed acquisition of [$^{18}$F]-FLT images since a dynamic acquisition (e.g. 2 h of acquisition) may not be realistic for routine clinical practice. It has been shown that [$^{18}$F]-FLT uptake occurs due to increased transport through the blood–brain barrier (BBB) and proliferation. When we focused on the condition for which the [$^{18}$F]-FLT tracer seemed to be relevant, i.e. the distinction between patients with grade III with CE and those with grade IV, all the tumors had an alteration of the BBB.

Although the advanced MRI and PET parameters show more and more interest and could become more accessible in the assessment of glioma (Heiss et al., 2011; Puttick et al., 2015), studies have often evaluated independently the interest of using either MRI or PET. In the present study, we benefit from the ability to compare the parameters from both advanced MRI and PET for each patient and illustrate their complementary role in glioma grading.

## 5. Conclusion

In conclusion, this study shows that [$^{18}$F]-FLT could be of interest in glioma classification particularly in differentiating grade IV glioblastoma from grade III or grade II gliomas. $FLT_{max}$ seems to be the best parameter to achieve this goal. Our work also illustrates the added value to acquire both, advanced MRI and [$^{18}$F]-FLT PET, to overcome the limitations of conventional imaging for doubtful patients.

## Conflicts of interest

The authors declare that they have no conflict of interest.

## Funding

This study was funded by the Institut National contre le Cancer (INCa), the Centre National de la Recherche Scientifique (CNRS), the Ministère de l'enseignement Supérieur et de la Recherche (MESR), the Université de Caen Basse-Normandie (UCBN), the Conseil Régional de Basse-Normandie (CRBN), the European Union — "Fonds Européen de Développement Régional" (FEDER), l'Europe s'engage en Basse-Normandie and the French National Agency for Research called "Investissements d'avenir" no. ANR-11-LABEX-0018-01. These sponsors were not involved in study design; in the collection, analysis and interpretation of data; in the writing of the report; and in the decision to submit the article for publication.

## Acknowledgments

We thank neurosurgeons E. Emery, S. Khoury, B. Gadan, and A. Borha. We also thank S. de Bouard, J. Pierre, S. Lecotcotigny and A. Manrique. We thank Valerie Fong for editing the article.

## References

Aronen, H.J., Gazit, I.E., Louis, D.N., Buchbinder, B.R., Pardo, F.S., Weisskoff, R.M., Harsh, G.R., Cosgrove, G.R., Halpern, E.F., Hochberg, F.H., et al., 1994. Cerebral blood volume maps of gliomas: comparison with tumor grade and histologic findings. Radiology 191 (1), 41–51. http://dx.doi.org/10.1148/radiology.191.1.81345968134596.

Arvinda, H.R., Kesavadas, C., Sarma, P.S., Thomas, B., Radhakrishnan, V.V., Gupta, A.K., Kapilamoorthy, T.R., Nair, S., 2009. Glioma grading: sensitivity, specificity, positive and negative predictive values of diffusion and perfusion imaging. J. Neurooncol. 94 (1), 87–96. http://dx.doi.org/10.1007/s11060-009-9807-619229590.

Chalkidou, A., Landau, D.B., Odell, E.W., Cornelius, V.R., O'Doherty, M.J., Marsden, P.K., 2012. Correlation between Ki-67 immunohistochemistry and $^{18}$F-fluorothymidine uptake in patients with cancer: a systematic review and meta-analysis. Eur. J. Cancer 48 (18), 3499–3513. http://dx.doi.org/10.1016/j.ejca.2012.05.00122658807.

Chen, W., Cloughesy, T., Kamdar, N., Satyamurthy, N., Bergsneider, M., Liau, L., Mischel, P., Czernin, J., Phelps, M.E., Silverman, D.H., 2005. Imaging proliferation in brain tumors with $^{18}$F-FLT PET: comparison with $^{18}$F-FDG. J. Nucl. Med. 46 (6), 945–95215937304.

Corroyer-Dulmont, A., Pérès, E.A., Petit, E., Guillamo, J.-S., Varoqueaux, N., Roussel, S., Toutain, J., Divoux, D., MacKenzie, E.T., Delamare, J., Ibazizène, M., Lecocq, M., Jacobs, A.H., Barré, L., Bernaudin, M., Valable, S., 2013. Detection of glioblastoma response to temozolomide combined with bevacizumab based on μMRI and μPET imaging reveals [$^{18}$F]-fluoro-L-thymidine as an early and robust predictive marker for treatment efficacy. Neuro-oncology 15 (1), 41–56. http://dx.doi.org/10.1093/neuonc/nos26023115160.

Dean, B.L., Drayer, B.P., Bird, C.R., Flom, R.A., Hodak, J.A., Coons, S.W., Carey, R.G., 1990. Gliomas: classification with MR imaging. Radiology 174 (2), 411–415. http://dx.doi.org/10.1148/radiology.174.2.21533102153310.

Derlon, J.M., Chapon, F., Noël, M.H., Khouri, S., Benali, K., Petit-Taboué, M.C., Houtteville, J.P., Chajari, M.H., Bouvard, G., 2000. Non-invasive grading of oligodendrogliomas: correlation between in vivo metabolic pattern and histopathology. Eur. J. Nucl. Med. 27 (7), 778–787. http://dx.doi.org/10.1007/s00259000026010952489.

Dhermain, F.G., Hau, P., Lanfermann, H., Jacobs, A.H., van den Bent, M.J., 2010. Advanced MRI and PET imaging for assessment of treatment response in patients with gliomas. Lancet Neurol. 9 (9), 906–920. http://dx.doi.org/10.1016/S1474-4422(10)70181-220705518.

Ferdová, E., Ferda, J., Baxa, J., Tupý, R., Mraček, J., Topolčan, O., Hes, O., 2015. Assessment of grading in newly-diagnosed glioma using $^{18}$F-fluorothymidine PET/CT. Anticancer Res. 35 (2), 955–95925667480.

Ginsberg, L.E., Fuller, G.N., Hashmi, M., Leeds, N.E., Schomer, D.F., 1998. The significance of lack of MR contrast enhancement of supratentorial brain tumors in adults: histopathological evaluation of a series. Surg. Neurol. 49 (4), 436–440. http://dx.doi.org/10.1016/S0090-3019(97)00360-19537664.

Hatakeyama, T., Kawai, N., Nishiyama, Y., Yamamoto, Y., Sasakawa, Y., Ichikawa, T., Tamiya, T., 2008. $^{11}$C-methionine (MET) and $^{18}$F-fluorothymidine (FLT) PET in patients with newly diagnosed glioma. Eur. J. Nucl. Med. Mol. Imaging 35 (11), 2009–2017. http://dx.doi.org/10.1007/s00259-008-0847-518542957.

Heiss, W.-D., Raab, P., Lanfermann, H., 2011. Multimodality assessment of brain tumors and tumor recurrence. J. Nucl. Med. 52 (10), 1585–1600. http://dx.doi.org/10.2967/jnumed.110.08421021840931.

Herminghaus, S., Pilatus, U., Möller-Hartmann, W., Raab, P., Lanfermann, H., Schlote, W., Zanella, F.E., 2002. Increased choline levels coincide with enhanced proliferative activity of human neuroepithelial brain tumors. N.M.R. Biomed. 15 (6), 385–392. http://dx.doi.org/10.1002/nbm.79312357552.

Hilario, A., Ramos, A., Perez-Nuñez, A., Salvador, E., Millan, J.M., Lagares, A., Sepulveda, J.M., Gonzalez-Leon, P., Hernandez-Lain, A., Ricoy, J.R., 2012. The added value of apparent diffusion coefficient to cerebral blood volume in the preoperative grading of diffuse gliomas. A.J.N.R. Am. J. Neuroradiol. 33 (4), 701–707. http://dx.doi.org/10.3174/ajnr.A284622207304.

Hutterer, M., Nowosielski, M., Putzer, D., Waitz, D., Tinkhauser, G., Kostron, H., Muigg, A., Virgolini, I.J., Staffen, W., Trinka, E., Gotwald, T., Jacobs, A.H., Stockhammer, G., 2011. O-(2-$^{18}$F-fluoroethyl)-L-tyrosine PET predicts failure of antiangiogenic treatment in patients with recurrent high-grade glioma. J. Nucl. Med. 52 (6), 856–864. http://dx.doi.org/10.2967/jnumed.110.08664521622893.

Idbaih, A., Ducray, F., Dehais, C., Courdy, C., Carpentier, C., de Bernard, S., Uro-Coste, E., Mokhtari, K., Jouvet, A., Honnorat, J., Chinot, O., Ramirez, C., Beauchesne, P., Benouaich-Amiel, A., Godard, J., Eimer, S., Parker, F., Lechapt-Zalcman, E., Colin, P., Loussouarn, D., Faillot, T., Dam-Hieu, P., Elouadhani-Hamdi, S., Bauchet, L., Langlois, O., Le Guerinel, C., Fontaine, D., Vauleon, E., Menei, P., Fotso, M.J.M., Desenclos, C., Verrelle, P., Verelle, P., Ghiringhelli, F., Noel, G., Labrousse, F., Carpentier, A., Dhermain, F., Delattre, J.-Y., Figarella-Branger, D., POLA Network, 2012. SNP array analysis reveals novel genomic abnormalities including copy neutral loss of heterozygosity in anaplastic oligodendrogliomas. P.L.O.S. ONE 7 (10), e45950. http://dx.doi.org/10.1371/journal.pone.004595023071531.

Idema, A.J.S., Hoffmann, A.L., Boogaarts, H.D., Troost, E.G.C., Wesseling, P., Heerschap, A., van der Graaf, W.T.A., Grotenhuis, J.A., Oyen, W.J.G., 2012. 3′-Deoxy-3′-$^{18}$F-fluorothymidine PET-derived proliferative volume predicts overall survival in high-grade glioma patients. J. Nucl. Med. Off. Publ. Soc. Nucl. Med. 53, 1904–1910. http://dx.doi.org/10.2967/jnumed.112.105544.

Jacobs, A.H., Thomas, A., Kracht, L.W., Li, H., Dittmar, C., Garlip, G., Galldiks, N., Klein, J.C., Sobesky, J., Hilker, R., Vollmar, S., Herholz, K., Wienhard, K., Heiss, W.-D., 2005. $^{18}$F-fluoro-L-thymidine and $^{11}$C-methylmethionine as markers of increased transport and proliferation in brain tumors. J. Nucl. Med. 46 (12), 1948–195816330557.

Jeong, S.Y., Lim, S.M., 2012. Comparison of 3′-deoxy-3′-[$^{18}$F]fluorothymidine PET and O-(2-[$^{18}$F]fluoroethyl)-L-tyrosine PET in patients with newly diagnosed glioma. Nucl. Med. Biol. 39, 977–981. http://dx.doi.org/10.1016/j.nucmedbio.2012.02.009.

Law, M., Yang, S., Babb, J.S., Knopp, E.A., Golfinos, J.G., Zagzag, D., Johnson, G., 2004. Comparison of cerebral blood volume and vascular permeability from dynamic susceptibility contrast-enhanced perfusion MR imaging with glioma grade. A.J.N.R. Am. J. Neuroradiol. 25 (5), 746–755515140713.

Law, M., Yang, S., Wang, H., Babb, J.S., Johnson, G., Cha, S., Knopp, E.A., Zagzag, D., 2003. Glioma grading: sensitivity, specificity, and predictive values of perfusion MR imaging and proton MR spectroscopic imaging compared with conventional MR imaging. A.J.N.R. Am. J. Neuroradiol. 24 (10), 1989–199814625221.

Lev, M.H., Ozsunar, Y., Henson, J.W., Rasheed, A.A., Barest, G.D., Harsh, G.R., Fitzek, M.M., Chiocca, E.A., Rabinov, J.D., Csavoy, A.N., Rosen, B.R., Hochberg, F.H., Schaefer, P.W., Gonzalez, R.G., 2004. Glial tumor grading and outcome prediction using dynamic spin-echo MR susceptibility mapping compared with conventional contrast-enhanced MR: confounding effect of elevated rCBV of oligodendrogliomas [corrected]. A.J.N.R. Am. J. Neuroradiol. 25 (2), 214–22114970020.

Louis, D.N., Ohgaki, H., Wiestler, O.D., Cavenee, W.K., Burger, P.C., Jouvet, A., Scheithauer, B.W., Kleihues, P., 2007. The 2007 WHO classification of tumours of the central

nervous system. Acta Neuropathol. 114 (2), 97–109. http://dx.doi.org/10.1007/s00401-007-0243-417618441.
Maia, A.C., Malheiros, S.M., da Rocha, A.J., da Silva, C.J., Gabbai, A.A., Ferraz, F.A., Stávale, J.N., 2005. MR cerebral blood volume maps correlated with vascular endothelial growth factor expression and tumor grade in nonenhancing gliomas. A.J.N.R. Am. J. Neuroradiol. 26 (4), 777–78315814920.
Miyake, K., Shinomiya, A., Okada, M., Hatakeyama, T., Kawai, N., Tamiya, T., 2012. Usefulness of FDG, MET and FLT-PET studies for the management of human gliomas. J. Biomed. Biotechnol. 2012, 205818. http://dx.doi.org/10.1155/2012/20581822577290.
Puttick, S., Bell, C., Dowson, N., Rose, S., Fay, M., 2015. PET, MRI, and simultaneous PET/MRI in the development of diagnostic and therapeutic strategies for glioma. Drug Discov. Today 20 (3), 306–317. http://dx.doi.org/10.1016/j.drudis.2014.10.01625448762.
Ricard, D., Idbaih, A., Ducray, F., Lahutte, M., Hoang-Xuan, K., Delattre, J.-Y., 2012. Primary brain tumours in adults. Lancet 379 (9830), 1984–1996. http://dx.doi.org/10.1016/S0140-6736(11)61346-922510398.
Riemenschneider, M.J., Jeuken, J.W., Wesseling, P., Reifenberger, G., 2010. Molecular diagnostics of gliomas: state of the art. Acta Neuropathol. 120 (5), 567–584. http://dx.doi.org/10.1007/s00401-010-0736-420714900.
Sadeghi, N., D'Haene, N., Decaestecker, C., Levivier, M., Metens, T., Maris, C., Wikler, D., Baleriaux, D., Salmon, I., Goldman, S., 2008. Apparent diffusion coefficient and cerebral blood volume in brain gliomas: relation to tumor cell density and tumor microvessel density based on stereotactic biopsies. A.J.N.R. Am. J. Neuroradiol. 29 (3), 476–482. http://dx.doi.org/10.3174/ajnr.A085118079184.
Schwarzenberg, J., Czernin, J., Cloughesy, T.F., Ellingson, B.M., Pope, W.B., Geist, C., Dahlbom, M., Silverman, D.H.S., Satyamurthy, N., Phelps, M.E., Chen, W., 2012. 3′-Deoxy-3′-$^{18}$F-fluorothymidine PET and MRI for early survival predictions in patients with recurrent malignant glioma treated with bevacizumab. J. Nucl. Med. Off. Publ. Soc. Nucl. Med. 53, 29–36. http://dx.doi.org/10.2967/jnumed.111.092387.
Scott, J.N., Brasher, P.M., Sevick, R.J., Rewcastle, N.B., Forsyth, P.A., 2002. How often are nonenhancing supratentorial gliomas malignant? A population study. Neurology 59 (6), 947–949. http://dx.doi.org/10.1212/WNL.59.6.94712297589.
Server, A., Kulle, B., Gadmar, Ø.B., Josefsen, R., Kumar, T., Nakstad, P.H., 2011. Measurements of diagnostic examination performance using quantitative apparent diffusion coefficient and proton MR spectroscopic imaging in the preoperative evaluation of tumor grade in cerebral gliomas. Eur. J. Radiol. 80 (2), 462–470. http://dx.doi.org/10.1016/j.ejrad.2010.07.01720708868.
Shin, J.H., Lee, H.K., Kwun, B.D., Kim, J.-S., Kang, W., Choi, C.G., Suh, D.C., 2002. Using relative cerebral blood flow and volume to evaluate the histopathologic grade of cerebral gliomas: preliminary results. A.J.R. Am. J. Roentgenol. 179 (3), 783–789. http://dx.doi.org/10.2214/ajr.179.3.179078312185064.
Sugahara, T., Korogi, Y., Kochi, M., Ikushima, I., Hirai, T., Okuda, T., Shigematsu, Y., Liang, L., Ge, Y., Ushio, Y., Takahashi, M., 1998. Correlation of MR imaging-determined cerebral blood volume maps with histologic and angiographic determination of vascularity of gliomas. A.J.R. Am. J. Roentgenol. 171 (6), 1479–1486. http://dx.doi.org/10.2214/ajr.171.6.98432749843274.
Van den Bent, M.J., 2010. Interobserver variation of the histopathological diagnosis in clinical trials on glioma: a clinician's perspective. Acta Neuropathol. 120 (3), 297–304. http://dx.doi.org/10.1007/s00401-010-0725-720644945.
Wester, H.-J., 2007. Nuclear imaging probes: from bench to bedside. Clin. Cancer Res. 13 (12), 3470–3481. http://dx.doi.org/10.1158/1078-0432.CCR-07-026417575209.
Yamamoto, Y., Ono, Y., Aga, F., Kawai, N., Kudomi, N., Nishiyama, Y., 2012. Correlation of $^{18}$F-FLT uptake with tumor grade and Ki-67 immunohistochemistry in patients with newly diagnosed and recurrent gliomas. J. Nucl. Med. 53 (12), 1911–1915. http://dx.doi.org/10.2967/jnumed.112.10472923081994.
Yang, D., Korogi, Y., Sugahara, T., Kitajima, M., Shigematsu, Y., Liang, L., Ushio, Y., Takahashi, M., 2002. Cerebral gliomas: prospective comparison of multivoxel 2D chemical-shift imaging proton MR spectroscopy, echoplanar perfusion and diffusion-weighted MRI. Neuroradiology 44 (8), 656–666. http://dx.doi.org/10.1007/s00234-002-0816-912185543.
Zonari, P., Baraldi, P., Crisi, G., 2007. Multimodal MRI in the characterization of glial neoplasms: the combined role of single-voxel MR spectroscopy, diffusion imaging and echo-planar perfusion imaging. Neuroradiol. 49 (10), 795–803. http://dx.doi.org/10.1007/s00234-007-0253-x17619871.
Zou, Q.-G., Xu, H.-B., Liu, F., Guo, W., Kong, X.-C., Wu, Y., 2011. In the assessment of supratentorial glioma grade: the combined role of multivoxel proton MR spectroscopy and diffusion tensor imaging. Clin. Radiol. 66 (10), 953–960. http://dx.doi.org/10.1016/j.crad.2011.05.00121663899.